# Use of Programmed Magnetic Bearing Stiffness and Damping to Minimize Rotor Vibration

J. M. KRODKIEWSKI AND R. B. ZMOOD

## ABSTRACT

This paper reports on recent work using magnetic bearings with programmed stiffness and damping for reducing rotor vibrations. It is shown that if these parameters are optimally programmed then the vibration amplitudes can be significantly reduced as the rotor passes through the critical speeds. In the example studied it is shown that the first two critical speed are completely suppressed while the third is significantly attenuated. The approach used is to determine the operating constraints of the bearing actuator and control system, and to then formulate an optimization problem which minimizes the rotor vibrations. This design methodology should also improve the robustness of the bearing system when subjected to external disturbances.

## INTRODUCTION

Vibration of rotors having slender shafts has been a troublesome and unremitting problem for designers of high speed machines over many years. Current trends toward machines having lower weight, smaller clearances, and higher speeds, in the interests of increased efficiency and lower cost, exacerbate these problems. As a result much attention has been devoted to methods of reducing vibration amplitudes using techniques such as squeeze–film dampers. Magnetic bearings, whose dynamic characteristics can be accurately varied over a broad range are an attractive alternative method to squeeze–film dampers for controlling vibrations, and interest in this approach has grown rapidly over recent years [1 – 4].

The earliest reported work on using a magnetic bearing for active vibration damping is by Schweitzer [5] where he proposed their use for damping self–excited rotor instabilities which arise because of internal rotor damping. He also suggested in this paper that magnetic bearings may be used to improve the operation of unbalanced rotors by damping the resonant peaks as the rotor passes through the critical speeds.

Gondhalekar et. al. [1], Allaire et.al. [3], and Salm [6] have reported on their work with an active magnetic bearing placed along the mid–shaft of a multi–disc

J.M.Krodkiewski, Department of Mechanical Engineering, The University of Melbourne, Victoria, Australia.

R.B.Zmood, Department of Communication and Electrical, Engineering, RMIT, Melbourne, Victoria, Australia

rotor. The control law considered by all authors was of the form $F_x = Kx + Cdx/dt$ where the coefficients $K$ and $C$ were held constant and independent of speed. Considerable reduction in the vibration amplitude at the higher critical speeds due to rotor unbalance forces was reported by all authors. Gondhalekar also observed that the critical speeds were altered by changes in the coefficient values.

Burrows and Sahinkaya [7], Bradfield et. al. [8] and Nonami et.al. [9] have also studied the use of active magnetic bearings placed along the mid–span of multi–disc rotors for damping vibrations. The control law was again of the form $F_x = Kx + Cdx/dt$, but the coefficients $K$ and $C$ were programmed to be a function of the rotor speed. Both Burrows and Bradfield reported on the vibrations experienced as the rotor speed increased from zero to above the first critical speed. In both cases the vibration amplitude was observed to be considerably reduced, especially in the region of the critical speed. Nonami has showed that the results observed by the first two authors extended to higher critical speeds where the vibration amplitudes also were reduced.

In all the approaches considered by the authors above the rotor continues to rotate about an axis which is displaced away from the principal inertia axis so that the unbalance forces continue to excite the rotor system. An alternative approach described by Haberman and Brunet [10, 11] which they have termed ACTIDYNE, and by Matsushita et.al. [4] uses a notch filter in the bearing feedback path with the notch frequency synchronized to the rotor speed. This results in the rotor experiencing no external forces at the frequency corresponding to the rotor speed. Thus the rotor will spin about the principal axis of inertia rather than the geometric axis.

Bradfield et.al. have identified a range of control strategies most clearly in [8]. One extreme of these control strategies is the approach taken in Refs. [4, 9] and [10] where the forces transmitted to the bearing support structures are to be minimized. At the other extreme is the case where the vibration amplitudes are to be minimized as considered by the earlier references. Burrows and Sahinkaya [2, 7] and Humphris et.al. [11] have examined an open loop technique for canceling rotor vibrations by introducing forces through the magnetic bearings which are synchronized with the shaft rotation. This technique does not involve alteration of the spring constant or damping of the magnetic bearing, but involves synchronous command signals being fed to the bearing axis control systems.

In this paper we report on recent work using magnetic bearings with programmed stiffness and damping for reducing rotor vibrations. This work shows that if these parameters are optimally programmed then the vibrations amplitudes can be significantly reduced when the rotor operates over a speed range containing several critical speeds. In this approach a non–linear model of the bearing actuator is developed and this is used to obtain a non–linear control law which results in an almost linear relationship between the bearing force and the journal displacement and velocity. The influence of the bearing control system constraints is obtained, and these are used in conjunction with a finite element model of the rotor to find the optimum bearing stiffness $K$ and damping coefficient $C$ for each rotor speed so as to minimize a cost function based on the rotor shape and applied bearing forces. The design methodology is used to compute the optimum values of $K$ and $C$ for an example of a multi–disc rotor.

## BEARING MODEL

The bearing force acting on the bearing journal is a function of the rotor position in the actuator bore, and the excitation current. In this analysis we will consider the case where the actuator has permanent magnets which generate a

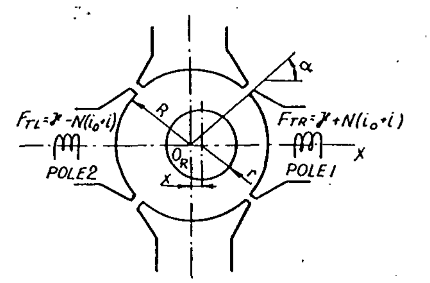


Figure 1. View of the bearing actuator.

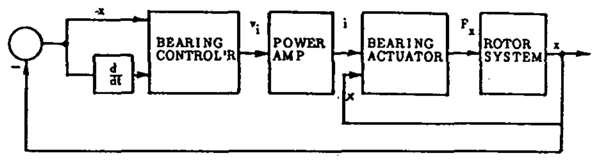


Figure 2. Bearing control system.

bias flux in the air–gap.

A number of simplifying assumptions will be made so that the analysis becomes tractable. Firstly it will be assumed the ferromagnetic poles and journal have infinite permeability and the permanent magnet MMF is uniform around the air–gap boundary. In addition the effects of flux fringing at the ends of the pole–faces will be accounted for by the fringing factor $k_f$, so that $t_{eff} = k_f t$, where $t_{eff}$ and $t$ are the effective and physical pole–face lengths respectively. It will also be assumed that the air–gap $c = R - r << R$, where $R$ is the actuator bore radius, $r$ is the journal radius, and all the pole–faces subtend the same angle $a$ about the axis $O_R X$. A cross–sectional view of the bearing actuator is shown in Fig. 1 for the case where the rotor is displaced a distance $x$ from the centre $O_R$ of the actuator bore.

We define the non–dimensional displacement $\bar{x} = x/c$, and the non–dimensional bias and control currents as $\bar{i}_0$ and $\bar{i}$ respectively, where

$$\bar{i}_0 = Ni_0/\mathcal{F} \qquad \text{and} \qquad \bar{i} = Ni/\mathcal{F}$$

with $i_0$ and $i$ being the respective bias and control currents, and $N$ is the number of turns on the control winding. In terms of these quantities it can be shown that the non–dimensional bearing force $\bar{F}_x(\bar{x}, \bar{i})$ is given by

$$\bar{F}_x(\bar{x}, \bar{i}) = \bar{\phi}_1(\bar{i}_0 + \bar{i})\bar{\psi}_1(\bar{x}) + \bar{\phi}_2(\bar{i}_0 + \bar{i})\bar{\psi}_2(\bar{x}) \tag{1}$$

where the non–dimensional force $\bar{F}_x$ is defined in terms of the bearing force $F_x$ by

$$\bar{F}_x(\bar{x}, \bar{i}) = F_x/\kappa\mathcal{F}^2 \tag{2}$$

Here

$$\bar{\phi}_1(\bar{i}) = (1 + \bar{i})^2, \qquad \phi_2(\bar{i}) = (1 - \bar{i})^2 \tag{3}$$

$$\psi_1(\bar{x}) = \frac{1}{1 - \bar{x}^2}\left[\frac{\sin a}{1 - \bar{x}\cos a}\right] + \frac{2\bar{x}}{(1 - \bar{x}^2)^{3/2}}\arctan\left[\sqrt{\frac{1 + \bar{x}}{1 - \bar{x}}}\tan\frac{a}{2}\right] \tag{4}$$

$$\psi_2(\bar{x}) = \frac{-1}{1 - \bar{x}^2}\left[\frac{\sin a}{1 + \bar{x}\cos a}\right] + \frac{2\bar{x}}{(1 - \bar{x}^2)^{3/2}}\arctan\left[\sqrt{\frac{1 - \bar{x}}{1 + \bar{x}}}\tan\frac{a}{2}\right] \tag{5}$$

and

$$\kappa = \left[\frac{R + r}{2}\right]\frac{\mu_0 t_{eff}}{c^2} \tag{6}$$

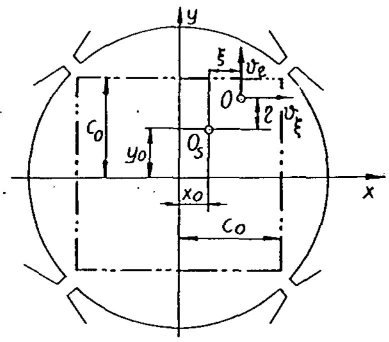

Figure 3. Position of the journal within operating clearance

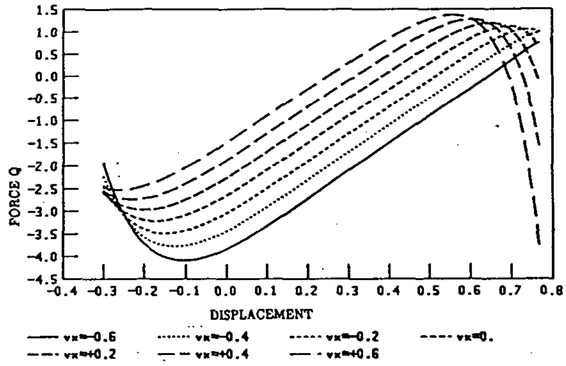

Figure 4. Dynamic characteristic $Q = -F(x, v_x)$ for $K = 6$ $C = 2$, $x_0 = 0.3$

## BEARING CONTROL SYSTEM

### CONTROL SYSTEM CONSTRAINTS

In addition to the operating constraints introduced by the bearing actuator considered above, the bearing control system also introduces further constraints which must be considered in magnetic bearing applications. These constraints have been considered from various perspectives by Burrows and Sahinkaya [7], and Maslen et. al. [13].

A block diagram for the bearing control system is shown in Fig. 2 where it can be seen that the journal displacement $\bar{x}$ is sensed and used as an input for the non–linear bearing controller. Its output $v_i$ is amplified in the power amplifier causing a current $i$ to flow in the bearing actuator which generates a journal force $F_x$. The maximum output current $i_{max}$ of the power amplifier is determined by the size of the amplifier output transistors. From this we see the output current $i(t)$ must satisfy $|i(t)| \leq i_{max}$. In Maslin et. al. [13] it has been shown that the current slew rate is limited by the power supply voltage so that $|di/dt| \leq (di/dt)_{max}$. These two constraints play a significant role in the analysis of the bearing controller which we now consider.

### CONTROL SYSTEM ANALYSIS

To maintain the bearing journal in the vicinity of the equilibrium point, denoted by $\bar{x}_0$, it is assumed the current $\bar{i}$ depends upon the journal position $\bar{\xi}$ and its instantaneous velocity $\bar{v}_\xi = d\bar{\xi}/d\bar{t}$, where non–dimensional time is defined in terms of the rotor speed $\omega$, by $\bar{t} = \omega t$, and the remaining parameters are defined in Fig. 3. Inspection of Fig. 2 shows that the coil current $i = i(\bar{\xi}, \bar{v}_\xi)$ is dependent upon the bearing controller transfer function which is chosen so that the force $\bar{F}$ given by Eq. (1) is a linear function of $\bar{\xi}$ and $\bar{v}_\xi$, namely $\bar{F} = K\bar{\xi} + C\bar{v}_\xi$.

Expanding $\bar{i}(\bar{\xi}, \bar{v}_\xi)$ into a Taylor series yields

$$\bar{i}(\bar{\xi}, \bar{v}_\xi) = \sum_{k=0}^{K} \sum_{l=0}^{L} \bar{a}_{kl} \bar{\xi}^k \bar{v}_\xi^l \tag{7}$$

and substituting Eq. (7) into Eq. (1) enables the coefficients $\bar{a}_{kl}$ to be computed for any desired bearing stiffness $K$ and damping coefficient $C$. As an example the coefficients $\bar{a}_{kl}$ for $k + l \leq 3$ have been computed for the magnetic bearing having the parameters given in Table 1 and with $K = 6$ and $C = 2$. Using these coefficients the dynamic characteristics of the bearing showing the force along the $x$-axis as a function of the displacement $x$ and velocity $v_x$ have been obtained by expanding Eq. (7) about the equilibrium point $x_0 = 0.3$. It can be seen from Fig. 4 that these characteristics are linear over a wide range about this point. The region where the bearing can be considered linear is called the operating clearance and is denoted by $\bar{c}_0$.

TABLE 1. - PARAMETERS OF THE MAGNETIC BEARING.

| Parameter Description | Symbol | Parameter Value |
|---|---|---|
| Stator–rotor air–gap | $c$ | 1.0 mm |
| Bearing actuator force coeff. | $\kappa$ | $1.49 \times 10^{-4}$ N/(A–t)$^2$ |
| Control winding turns | $N$ | 140 turn |
| Perm. magnet air–gap MMF | $\mathcal{F}$ | 299 A–t |
| Pole face angle | $\alpha$ | 45 deg |
| Max. cont. wdg. current | $i_{max}$ | 2 A |
| Max. cont. wdg. curr. slew rate | $di/dt_{max}$ | 5000 A/sec |
| Actuator saturation current | $i_{sat}$ | 3 A |
| Bias current | $i_0$ | 0 A |

## PERMISSIBLE STIFFNESS AND DAMPING COEFFICIENTS

At each instant the currents $(1 + \bar{i}_0 + \bar{i})$ and $(1 - \bar{i}_0 - \bar{i})$ must satisfy the inequalities

$$i_{min} \leq (1 + i_0 + i) \quad \text{and} \quad (1 - i_0 - i) \leq i_{sat} \tag{8}$$

The lower bound ensures that no flux reversal occurs in the bearing airgap while the upper bound ensures that the iron components in the bearing always remain unsaturated. Within the operating clearance $c_0$ the bearing force is linear so if a harmonic motion of the journal exists having frequency $\omega$ and amplitude less than $c_0$ then the generated force is also a harmonic function. The largest harmonic motion in this case is thus given by

$$\xi(t) = c_0 \sin \omega t \tag{9}$$

where $\omega$ is the shaft speed of rotation. Combining Eqs. (7), (8), and (9) indicates that the coefficients $\bar{a}_{kl}$ are constrained by the limits $i_{min}$, and $i_{sat}$. This in turn implies limits on the coefficients $K$ and $C$. These are illustrated in Fig. 5 for a bearing having the parameters given in Table 1. The ticks on this figure indicate the regions of permissible values for the parameters $K$ and $C$.

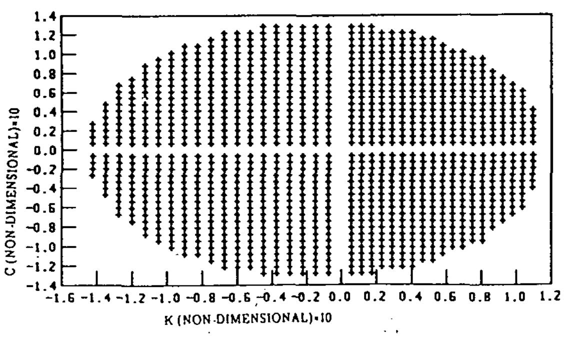


Figure 5. Range of available K & C for $c_0$=0.2, $x_0$=0.3.

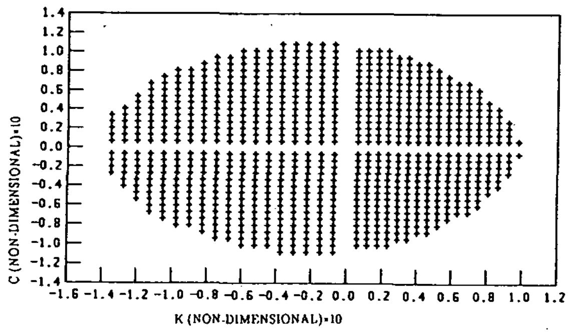


Figure 6. Range of available K & C for $c_0$=0.2, $x_0$=0.3, $\nu$=0.78

When the effect of the current slew rate is included in the analysis the region of permissible values for $K$ and $C$ is further restricted from that arrived at in Fig. 5, and is shown in Fig. 6. The apparent difference between the achievable positive stiffness and negative stiffness is due to the effect of the permanent magnet field.

## OPTIMIZATION OF ROTOR–BEARING SYSTEM

### MATHEMATICAL MODEL OF ROTOR–BEARING SYSTEM

We consider the example shown in Fig. 7 having a total mass $m_r$ = 2.98 kg, where the rotor is supported at nodes 2 and 3 by identical magnetic bearings. From our earlier analysis the bearing forces in the $x$ and $y$ directions can be expressed as

$$\{F^x_{br}\} = [c^x_b]\,\dot{\xi}_b + [k^x_b]\,\xi_b \tag{10}$$

and

$$\{F^y_{br}\} = [c^y_b]\,\dot{\eta}_b + [k^y_b]\,\eta_b \tag{11}$$

where $[k^{x,y}_b]$ are the bearing stiffness matrices and $[c^{x,y}_b]$ are the bearing damping coefficient matrices. Using finite element methods the equations of motion for the rotor–bearing system can be shown to be

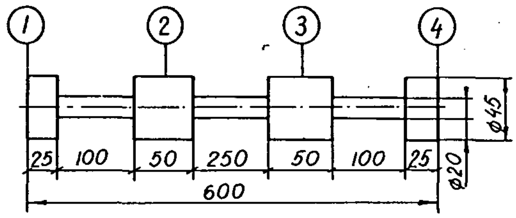


Figure 7. Rotor of the system.

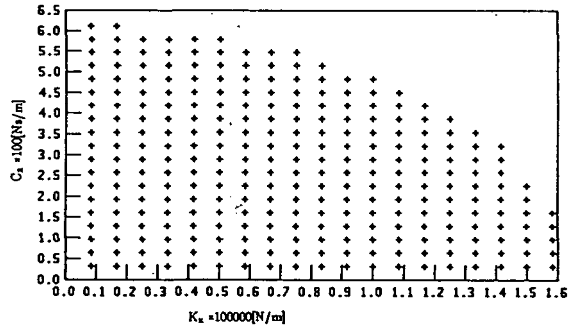


Figure 8. Range of available $K_x$ and $C_x$ for $\omega$=300 rad/s and $x_0$=0.35

$$[m_T]\{\ddot{\xi}\} + [c_b^{\xi}]\{\dot{\xi}\} + ([k_T] + [k_b^{\xi}])\{\xi\} = \{F_{ex}\} \tag{12}$$

$$[m_T]\{\ddot{\eta}\} + [c_b^{\eta}]\{\dot{\eta}\} + ([k_T] + [k_b^{\eta}])\{\eta\} = \{F_{ex}\} \tag{13}$$

For satisfactory operation of the rotor–bearing system the solutions of Eqs. (12) and (13) must be stable which implies that their eigenvalues must have negative real parts. The domain of the coefficients $K$ and $C$ for which solutions of Eq. (12) are stable is shown in Fig. 8 for $\omega$ = 300 rad/sec. Similar plots can be constructed for different speeds of rotation, and also for the $y$–axis bearing described by Eq. (13).

## OPTIMIZATION OF COEFFICIENTS *K* AND *C*.

Equations (12) and (13) can be solved for forced excitation such as occurs when the rotor is unbalanced. In this case the excitation can be represented in phasor form

$$\{F_{ex}\} = \{F_{ex0}\}\, e^{i\omega t} = [m_T]\{\mu\}\, \omega^2 e^{i\omega t} \tag{14}$$

where $\{\mu\}$ is the vector of rotor residual unbalance. For simplicity it has been assumed that $\{\mu\}$ is a linear combination of the natural free–free modes of the rotor so that $\{\mu\}^T = \{\, 2, -0.38, 1.89, 2\}$.

The complex amplitude responses of the forced vibrations can be obtained from Eqs. (12), (13), and (14), and are given by

$$\{A_{\xi}\} = \left[[m_T]\, \omega^2 + [c_b^{\xi}]i\omega + [k_b^{\xi}]\right]^{-1}\{F_{ex0}\} \tag{15}$$

$$\{A_{\eta}\} = \left[[m_T]\, \omega^2 + [c_b^{\eta}]i\omega + [k_b^{\eta}]\right]^{-1}\{F_{ex0}\} \tag{16}$$

In formulating the optimization problem it has been assumed that the goal is to seek the optimum values for the coefficients $K$ and $C$ which minimize a functional defined along the length of the rotor. As observed by Bradfield et. al. [8] this functional can be defined in many ways. In this work we have taken the

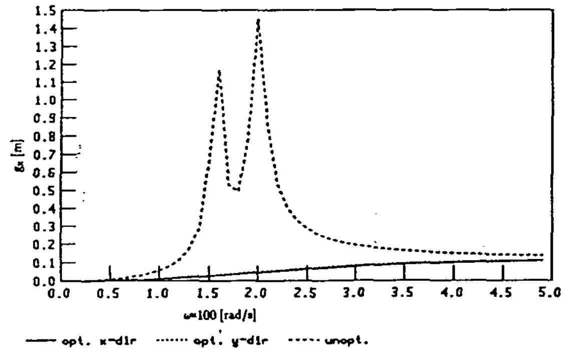


Figure 9. Objective function for $c_0$=0.2, $\omega$=10-500 rad/s

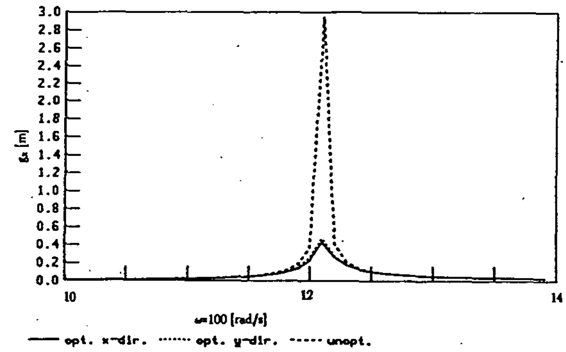


Figure 10. Objective function for $c_0$=0.2, $\omega$=1000-1400 rad/s

objective function as

$$g_x(K^x, C^x) = \sqrt{\frac{1}{4}\sum_{i=1}^{4} |A_{\xi i}|^2} \tag{17}$$

$$g_y(K^y, C^y) = \sqrt{\frac{1}{4}\sum_{i=1}^{4} |A_{\eta i}|^2} \tag{18}$$

In this case the goal is to minimize the peak mean squared magnitude of the vibration amplitudes along the rotor. An alternative goal might be to include weighting functions in Eqs. (17) and (18) which weight vibrations at certain locations differently from others. Other useful functionals might be to measure the vibration forces transmitted to the bearing supports. In this case the goal could be to select the $K$ and $C$ coefficients so that the transmitted forces are zero, in which case the rotor would be rotating about its principal axis of inertia.

## SOME COMPUTATIONAL RESULTS

Computation shows the objective function (17) has its global minimum subject to the constraints defined by Fig. 8 for $\omega$ = 300 rad/sec, when $K^x$ = 6040 N/m and $C^x$ = 648 N s/m. Similar results are obtained for the $y$-axis. Having obtained the optimum $K^x$ and $C^x$ the coefficients $\bar{a}_{kl}$ can be determined using the Eq. (7) to obtain the optimum control law for the given speed. To obtain the optimum control law for other rotor speeds these computations can be repeated for each speed. The results of these computations are shown in Figs. 9 to 11.

In Figs. 9 and 10 the object function of the system is presented for speeds up to the third critical speed. For comparison the object function for the same rotor is presented where it is supported by two bearings having constant stiffness $K$ = 6000 N/m and damping $C$ = 20 N.s/m. It will be noted that the unoptimized system has three critical speeds at approximately 160, 210, and 1120

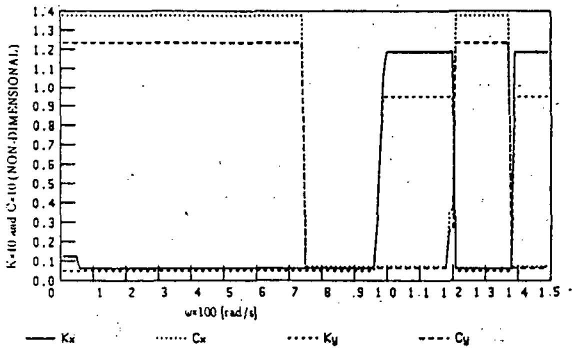


Figure 11. Non-dimensional optimal coefficients K and C for $c_0$=0.2

rad/sec. At the two lowest speeds the optimized system shows no vibration resonance whatsoever. At the third critical speed the optimized system has a small resonance, but it is attenuated by about 17 dB compared with the unoptimized system.

In Fig. 11, the optimum stiffness $K^x$, $K^y$ and damping coefficients $C^x$, $C^y$ are plotted as a function of speed. It will be observed that these coefficients vary over a wide range as the speed is increased, and that while at some speeds high stiffness and low damping is required, at other speeds the converse is necessary, and yet, at other speeds both low stiffness and damping is required to minimize the objective function.

## CONCLUSIONS

In this approach to the design of magnetic bearing rotor systems we have attempted to choose optimum values for the parameters $K$ and $C$ which minimize the shaft vibrations by minimizing a functional defined along the length of the shaft. It is shown that the optimum values for $K$ and $C$ depend upon the rotor speed so that they need to be programmed for optimum performance of the rotor system. By using the programmed values for the parameters it has been shown that the resonances at the rotor critical speeds can be eliminated or very heavily suppressed.

Since the design methodology guarantees optimum performance for all points inside the region defined by the optimum clearance $c_0$, which is of finite size, this approach should lead to robust performance of these systems when subjected to substantial disturbances.

## REFERENCES

1. Gondehalekar, V, Holmes R.,"Design of a Radial Electromagnetic Bearing for the Vibration Control of a Supercritical Shaft", Proc Instn Mech Engr, Vol 198 C (1984) pp 331–336

2. Burrows, C.R., Sahinkaya, M.N., "Vibration Control of Multi–Mode Rotor–Bearing Systems" Proc R Soc London, Vol A 386, (1983) pp 77–94.

3. Allaire, P.E., Kasarda M.E.F.,Humphris, R.R., Lewis D.W., "Vibration Reduction in a Multimass Flexible Rotor Using a Midspan Magnetic Damper", Proc First Internat. Symp. on Magnetic Bearings, Zurich, Switzerland, June 6–8, 1988.

4. Matsushita,O., Yoshida, J., Takahashi, N., "Rotor Vibration Simulation Method for Active Magnetic Bearing Control", Proc Second Internat Symp on Magnetic Bearings, Tokyo, Japan, July 12–14, 1990.

5. Schweitzer, G., " Stabilization of Self–Exccited Rotor Vibrations by an Active Damper", in Dynamics of Rotors, F.J. Mordson, ed., Springer–Verlag, Berlin 1975, pp 472–492.

6. Salm, J.R., "Active Electromagnetic Suspension of an Elastic Rotor : Modelling, Control, and Experimental Results", 1987 ASME Design Technical Conf.11th Biennial Conf on Mech Vibrations and Noise, Boston, Mass, Sept 27–30. 1987, pp 141–149.

7. Burrows, C.R., Sahinkaya, M.N., " Control Strategies for Use with Magnetic Bearings", Proc Internat. Conf. on Vibrations in Rotating Machinery, (publ. Inst. Mech. Engrs.) Heriot–Watt University, Edinburgh, Sept. 13–15, 1988, pp 23–32.

8. Bradfield, C.D., Roberts, J.B., Karunendiran, S., " A Programmable Electromagnetic Bearing for Vibration Control of a Flexible Shaft",1989 ASME Design Technical Conf - 12th Biennial Conf. on Mech. Vibrations and Noise, Montreal, Quebec, Sept 17–21,1989.

9. Nonami, K., Yamaguchi H., Active Vibration Control of Flexible Rotor for High Order Critical Speeds using Magnetic Bearings, Proc Second Internat. Symp. on Magnetic Bearings, July 12–14, 1990, Tokyo, Japan.

10. Haberman, H., Brunet, M., " The Active Magnetic Bearing Enables Optimum Damping of Flexible Rotor", ASME Internat. Gas Turbine Conf. ,March 1984 Paper 84–GT–117.

11. Haberman, H., Brunet, M., " The Active Magnetic Bearing Enables Optimum Control of Machine Vibrations", ASME Internat. Gas Turbine Conf. March 18–21, 1985, Paper 85–GT–221

12. Humphris, R.R., Knospe, C.R., Sundaram, S.," Dynamic Balancing with Open Loop Control of Magnetic Bearings", Proc. 26th Intersoc. Energy Conversion Engineering Conf., Boston, Mass. Aug 4–9, 1991, pp 192–197.

13. Maslen, E., Hermann, P., Scott, M., Humphris, R.R., "Practical Limits to the Performance of Magnetic Bearings: PeakForce, Slow Rate, and Displacement Sensitivity", Trans.ASME, Jnl of Tribology, Vol 111 (Apr 1989) pp 331–336.